Journal of Industrial and Engineering Chemistry 80 (2019) 527–534

Contents lists available at ScienceDirect

Journal of Industrial and Engineering Chemistry

journal homepage: www.elsevier.com/locate/jiec

Development of high-performance membrane-electrode assembly in unitized regenerative fuel cells

Ji Eun Park[a,b,1], Mohanraju Karuppannan[c,1], Oh Joong Kwon[c,*], Yong-Hun Cho[d,**], Yung-Eun Sung[a,b]

[a] Center for Nanoparticle Research, Institute for Basic Science (IBS), Seoul 08826, Republic of Korea
[b] School of Chemical and Biological Engineering, Seoul National University, Seoul 08826, Republic of Korea
[c] Department of Energy and Chemical Engineering, Incheon National University, 12-1, Songdo-dong, Yeonsu-gu, Incheon 22012, Republic of Korea
[d] Department of Chemical Engineering, Kangwon National University, Samcheok, Kangwon-do 25913, Republic of Korea

ARTICLE INFO

Article history:
Received 8 April 2019
Received in revised form 6 August 2019
Accepted 12 August 2019
Available online 20 August 2019

Keywords:
Unitized regenerative fuel cell
Membrane-electrode assembly
Oxygen electrode
Oxygen reduction reaction
Oxygen evolution reaction

ABSTRACT

In this work, we investigated the membrane-electrode assembly (MEA) parameters of an oxygen electrode to develop a high-performance unitized regenerative fuel cell (URFC) that can be operated in fuel cell (FC) and water electrolysis (WE) mode. The MEA parameters including gas diffusion layer, ionomer content, oxygen reduction reaction (ORR) type, oxygen evolution reaction (OER) catalyst, and catalyst loading were optimized by calculating the round-trip efficiency of URFC. The performance in FC mode was largely affected by the MEA parameters compared to that of the WE mode performance. The FC mode performance is crucial for the achievement of high URFC performance. The optimized round-trip efficiency was 49% at 500 mA cm^{-2}, which is comparable or superior to that reported in literature. This result can be attributed to the highly efficient MEA structure suitable for bifunctional catalysts to participate in both ORR and OER.

Introduction

A unitized regenerative fuel cell (URFC) integrating a fuel cell (FC) and water electrolysis (WE) in single cell is an attractive energy conversion and storage device [1,2]. In WE mode, the water is split into hydrogen and oxygen using electrical energy. Subsequently, the generated hydrogen and oxygen can be used as reactants for the fuel cell, producing electricity when the URFC is operated in FC mode. URFCs exhibit high specific energy due to their solid electrolytes and good durability when compared with secondary and redox flow batteries [1]. However, URFCs exhibit low round-trip efficiencies of 40–50% compared to other energy storage devices due to the sluggish kinetics of the oxygen electrocatalysts. Moreover, noble metals such as platinum (Pt), iridium (Ir), ruthenium (Ru), or their alloys are typically used as electrocatalysts in the oxygen electrode, leading to high costs [3–5].

Research regarding performance enhancement has been reported to improve the abovementioned drawbacks. Various bifunctional catalysts that exhibit good oxygen reduction reaction (ORR) and oxygen evolution reaction (OER) activities, including PtIr alloys [6–8], PtRu alloys [6], (RuO_2–IrO_2)/Pt [9], and Pt/IrO_2 [10] have been used as oxygen electrodes in URFCs. Yim et al. [6] prepared oxygen electrodes with different noble metals and alloy catalysts, i.e. PtIr, PtIrOx, PtRu, PtRuOx, PtRuIr, and Pt black. Among the prepared catalysts, the PtIr alloy with 1% Ir showed the highest URFC performance of 47% at 500 mA cm^{-2}. Zhang et al. [9] proposed deposited RuO_2–IrO_2 on a Pt black catalyst to form a bifunctional catalyst in a URFC. The URFC prepared using this catalyst exhibited higher performance and durability than obtained using a mixture of RuO_2–IrO_2 and Pt black catalyst. Lee et al. [10] synthesized the deposited Pt/IrO_2 on porous carbon paper and reduced the catalyst loading to 0.4 mg cm^{-2}. In the oxygen electrode, the porous Pt structure on the IrO_2 layer prevented inhibition of the electrochemical reaction of the sublayer IrO_2, resulting in high URFC performance.

Additionally, oxygen electrode structures have been modified using mixtures of commercial Pt- and Ir-based catalysts [11,12].

* Corresponding author at: Department of Energy and Chemical Engineering, Incheon National University, 12-1, Songdo-dong, Yeonsu-gu, Incheon 22012, Republic of Korea.
** Corresponding author at: Department of Chemical Engineering, Kangwon National University, Samcheok, Kangwon-do 25913, Republic of Korea.
E-mail addresses: ojkwon@inu.ac.kr (O.J. Kwon), yhun00@kangwon.ac.kr (Y.-H. Cho).
[1] JEP and MK contributed equally to this work.

https://doi.org/10.1016/j.jiec.2019.08.029
1226-086X/

Altmann et al. [11] reported the effects of oxygen electrode configuration effects on URFC performance. Three configurations, mixture, multilayer, and segmented electrodes, were adopted using Pt and IrO_2. The URFC consisting of mixed Pt and IrO_2 exhibited the highest performance, as interfacial contact to the membrane is crucial. However, this mixed electrode showed poor cyclic performance. Lee et al. [12] developed an IrO_2/Pt/IrO_2 multilayer electrode and achieved good cyclic performance, exhibiting a high round-trip efficiency of 48% at 500 mA cm^{-2}. In addition, the Pt layer was separated with GDL in the electrode structure, preventing carbon corrosion of GDL and showing high cyclability without performance loss.

The optimization of membrane-electrode assembly (MEA) components is important for enhancing URFC performance. In electrochemical devices consisting of polymer-electrolyte membranes (PEMs), such as polymer-electrolyte membrane fuel cells (PEMFCs) and polymer-electrolyte membrane water electrolysis (PEMWE), the MEA preparation significantly influences cell performance [13–15]. In addition, PEMFC and PEMWE require different MEA parameters to achieve optimal performance. As the URFC is a unitized cell that combines PEMFC with PEMWE, it is necessary to develop novel MEA parameters that are suitable for URFC. However, few studies focusing on these MEA parameters have been reported in the literature. Thus, the investigation of MEA parameters is crucial for the development of high-performance URFCs using bifunctional catalysts in the oxygen electrode.

Herein, we developed a novel MEA structure to achieve high initial URFC performance by combining the catalytic activity of various bifunctional catalysts in a practical device. Although carbon-based materials can be corroded under WE mode, we used these materials in URFC to attain high initial performance. It is because URFC prepared with titanium-based materials showed low FC performance and low round-trip efficiency due to hydrophilicity of titanium-based materials. Therefore, the MEA parameters including the GDL, Nafion content, catalyst loading, as well as ORR and OER catalyst types, were adjusted to obtain optimal round-trip efficiency.

Experimental

URFC assembly

Fig. 1 shows a schematic diagram of the oxygen electrode used in URFCs. A single cell is comprised of the MEA, which consists of a membrane and two catalyst layers (anode and cathode) as well as two gas diffusion layers (GDLs). The MEAs were prepared using the catalyst-coated membrane (CCM) method reported previously [16,17]. Nafion 212 (Dupont, USA) was used as the polymer-electrolyte membrane. The anode catalysts were 40 wt% Pt/C with loadings of 0.2 mg_{Pt} cm^{-2}. The cathode catalysts were mixtures of Pt-based materials (Pt black as well as 60, 40, and 20 wt% Pt/C (Johnson Matthey Co., USA) as an ORR catalyst and Ir-based materials (IrO_2 (Surepure Chemetals Co., USA) and Ir (Alfa Aesar Co., USA)) as an OER catalyst with a weight ratio of Pt to Ir of 1:1. The loading and type of ORR and OER catalyst in the cathode were optimized and discussed further in Sections “Effect of Nafion content in oxygen electrode”, “Effect of ORR catalyst in oxygen elecrode”, and “Effect of OER catalyst in oxygen electrode”. The catalyst layers were fabricated with the catalyst, Nafion ionomer (Aldrich Chem. Co., USA), isopropyl alcohol, and deionized water. Two catalyst slurries (anode and cathode) were sprayed onto each side of the membrane. Subsequently, the GDLs were placed on both sides of the CCM and the three GDLs were optimized: A3-20, A3-30, and A3-40 (JNTG20-A3, JNTG30-A3, JNTG40-A3, JNTG Co., Republic of Korea).

Electrochemical characterization

The URFC performance in fuel cell (FC) mode was measured in an active area of 5 cm^2. The test was performed under a fully humidified H_2–O_2 atmosphere at an ambient pressure. The flow rates of H_2 and O_2 were both 100 mL min^{-1} and the cell temperature was maintained at 75 °C. FC tests were evaluated using the current sweep method at 10 mA cm^{-2} s^{-1} with load cycling from the open-circuit voltage to 0.35 V.

To determine the URFC performance in water electrolysis (WE) mode, preheated water (50 °C) was allowed to flow into the anode side with a constant flow rate of 1 mL min^{-1}. Before operation, the preheated water was fed for 10 min to supply sufficient reactant to the catalyst layer. The cell temperature was maintained at 75 °C and single cell tests were performed using the voltage sweep method with load cycling from 1.25 to 2.05 V at 2 mV s^{-1}.

URFC performance was evaluated using the round-trip efficiency between FC and WE modes. The round-trip efficiency was calculated by dividing the cell voltage in FC mode by that observed in WE mode at constant current density of 500 mA cm^{-2}. To characterize the resistance in the FC and WE modes of the URFC, electrochemical impedance spectra (EIS) (IM-6, ZAHNER-elektrik GmbH & Co. KG, Germany) were obtained at –500 (FC mode) and 500 mA cm^{-2} (WE mode) with frequencies ranging from 100 mHz to 100 kHz.

FE-SEM characterization

The catalyst layer morphologies were examined using field-emission scanning electron microscopy (FE-SEM, SUPRA 55UP, Carl Zeiss, Germany). In addition, the catalyst layer thicknesses were measured using FE-SEM after sample preparation. The MEAs were sectioned to allow for observation of their cross-sections using liquid nitrogen.

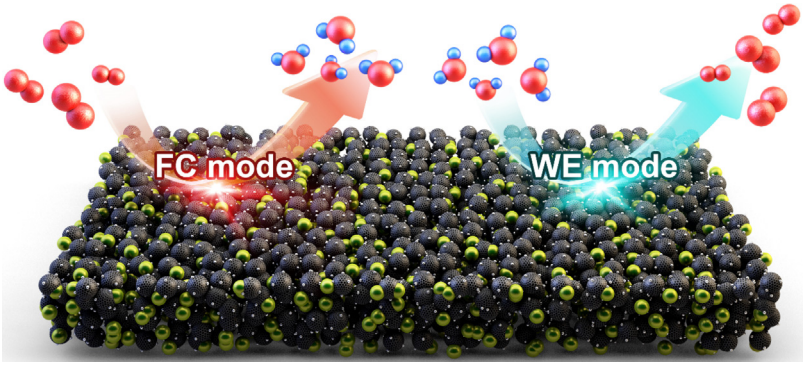

Fig. 1. Schematic representation of the oxygen electrode in a URFC.

Results and discussion

The effect of the GDLs in the two electrodes

GDLs, which were placed between the catalyst layer and bipolar plates, were composed of porous material (carbon nanofibers). They provide pathways for electrons, reactants, and water, affecting the mass transport resistance of the PEMFC and PEMWE [18,19]. In PEMFC, the SGL 35BC GDL (SGL group, Germany) is commonly used as a GDL [20,21]. This material is carbon paper with a polytetrafluorethylene (PTFE) content of 5 wt%, a microporous layer (MPL), and thickness of 320 μm. In contrast, thicker GDLs are generally used in PEMWE [22]. Thus, the examination of GDL thickness is essential for determination of the optimal GDL in URFC, which operates in both FC and WE modes.

Fig. 2 shows the polarization curves of the URFCs prepared with different GDL thicknesses (A3-20 (270 μm), A3-30 (320 μm) and A3-40 (420 μm)). In WE mode (Fig. 2(a)), the cell performance in the overall current densities region increased with increased GDL thickness (A3-40 > A3-30 > A3-20) due to improved contact between the catalyst layer and GDL. However, at 500 mA·cm^{-2} the performances of the samples prepared with A3-30 and A3-40 were approximately the same. On the other hand, the FC mode results (Fig. 2(b)) showed the highest cell performance for the A3-30 sample. Unlike in WE mode, the thicker GDL thickness did not lead to improved FC performance, which can be attributed to decreased mass transport of the reactants and products. When the round-trip efficiency was calculated by dividing the FC performance by WE performance at 500 mA cm^{-2}, the A3-30 URFC exhibited the highest efficiency of 46.3%. Thus, the optimal GDL was determined to be A3-30 and was used for the following experiments.

Effect of catalyst loading of the oxygen electrode

Catalyst loading of the oxygen electrode is crucial for URFC performance. When catalyst loading is increased, the cell performance generally increases due to the increased number of active sites. However, for URFCs using a solid electrolyte, the catalyst layer thickness can decrease cell performance as a thicker layer decreases the mass transport of reactants and products [23]. Therefore, the catalyst loading was optimized to obtain high performance. Fig. 3(a, d) shows the polarization curves of the URFCs prepared with different catalyst loadings of 0.2, 0.4, 1.0, and 2.0 mg cm^{-2} in FC and WE mode. For both modes, the cell performance at 500 mA cm^{-2} was enhanced with increasing catalyst loading from 0.2 to 1.0 mg cm^{-2}. This enhancement can be attributed to the increased number of active sites, which have activity for the ORR and OER. At 2.0 mg cm^{-2} loading, the performance decreased in both FC and WE modes due to the thicker catalyst layer inducing increased mass transport resistance. From Fig. 3(b–f), the SEM images show the thickness of catalyst layers with catalyst loadings of 0.2, 0.4, 1.0, and 2.0 mg cm^{-2}. The thicknesses of the four MEAs were 2.34, 6.35, 15.53, and 37.07 μm. When the catalyst loading was 2.0 mg cm^{-2}, the excessively thick catalyst layer significantly affected mass transport and cell performance. As a result, the optimum catalyst loading was 1.0 mg cm^{-2}, exhibiting a high round-trip efficiency of 47%.

Effect of the Nafion content in the oxygen electrode

The Nafion ionomer is a proton-conductor which provides an ionic pathway from the membrane to catalysts [24,25]. Low Nafion ionomer contents are insufficient to properly conduct ions (protons) in the catalyst layer and excessively high contents can block active sites, leading decreased cell performance [26]. The effect of Nafion content on the PEMFC performance has been reported by Passalacqua et al. [27] and Suzuki et al. [28]. These authors showed that 33 wt% was the optimal content in the PEMFC cathode. In addition, Wu and Scott [29] investigated the Nafion ionomer in PEMWE, showing that the optimized content of Nafion was 25 wt%. Thus, the Nafion content in the oxygen electrode was examined to determine the optimal ionomer content for URFCs operated in both FC and WE modes.

In this study, Nafion contents of 10, 20, 30, and 40 wt% were used in catalyst layer of the oxygen electrode. As shown in Fig. 4(a), the performance of the four MEAs at 500 mA·cm^{-2} were largely similar (1.6 V) in WE mode. In the high current density region, increased Nafion contents resulted in slightly increased performance, whereas the Nafion content in FC mode significantly affected cell performance (Fig. 4(d)). The MEA with Nafion content of 30 wt% exhibited the highest performance. The cell voltages of the four MEAs (10, 20, 30, and 40 wt% Nafion) at 500 mA cm^{-2} were 0.654, 0.706, 0.74, and 0.731 V, respectively. Thus, the corresponding round-trip efficiencies were 40.6, 43.8, 46.3, and 45.5%, respectively, showing that 30 wt% was the optimal Nafion content in the URFC. Fig. 4(b–f) shows the SEM images of the catalyst layers with different Nafion contents. From the SEM images, the Nafion content determined the proton conductivity and the formation of secondary pores in the catalyst layer. That is, when 30 wt% Nafion was applied, the catalyst exhibited the optimal morphology for high performance and was used for further experiments.

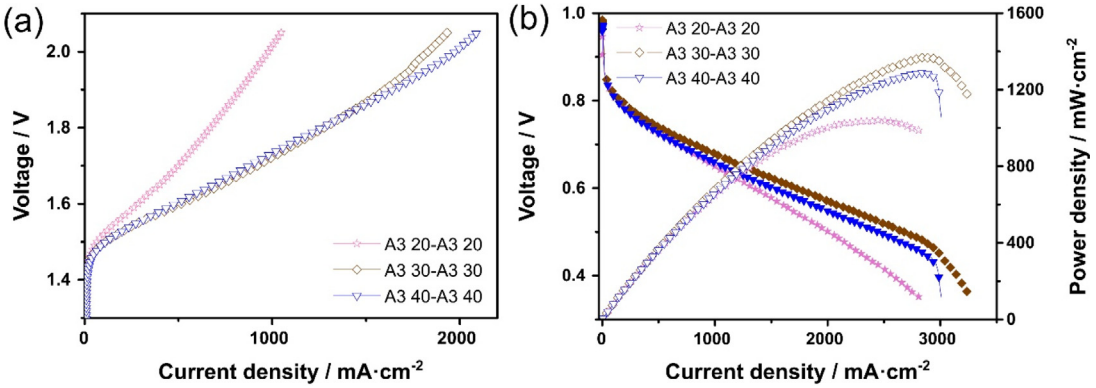

Fig. 2. Polarization curves of URFCs using three gas diffusion layers (GDLs) with various thicknesses (A3-20 (270 μm), A3-30 (320 μm), and A3-40 (420 μm). (a) WE mode and (b) FC mode. The catalyst loading was 0.4 mg cm^{-2} and cell temperature was 75 °C.

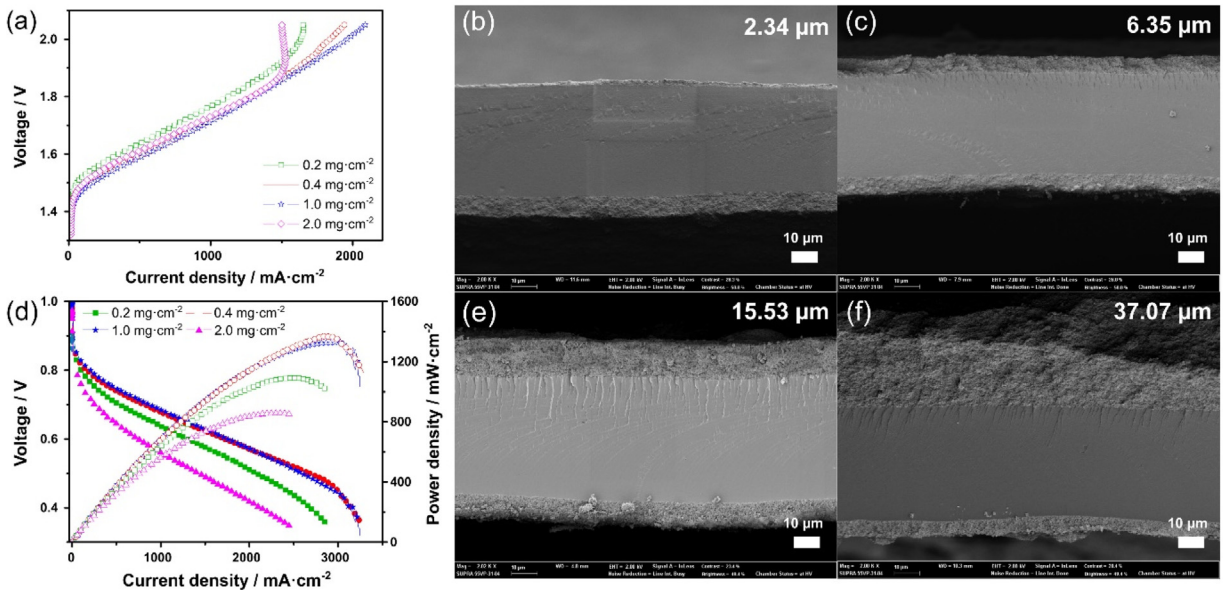

Fig. 3. The effect of catalyst loading (a, d) polarization curves of the URFCs prepared using different catalyst loadings in the oxygen electrode in (a) WE and (d) FC mode and (b–f) FE-SEM images of the MEA with catalyst loadings of (b) 0.2, (c) 0.4, (e) 1.0, and (f) 2.0 mg cm^{-2}.

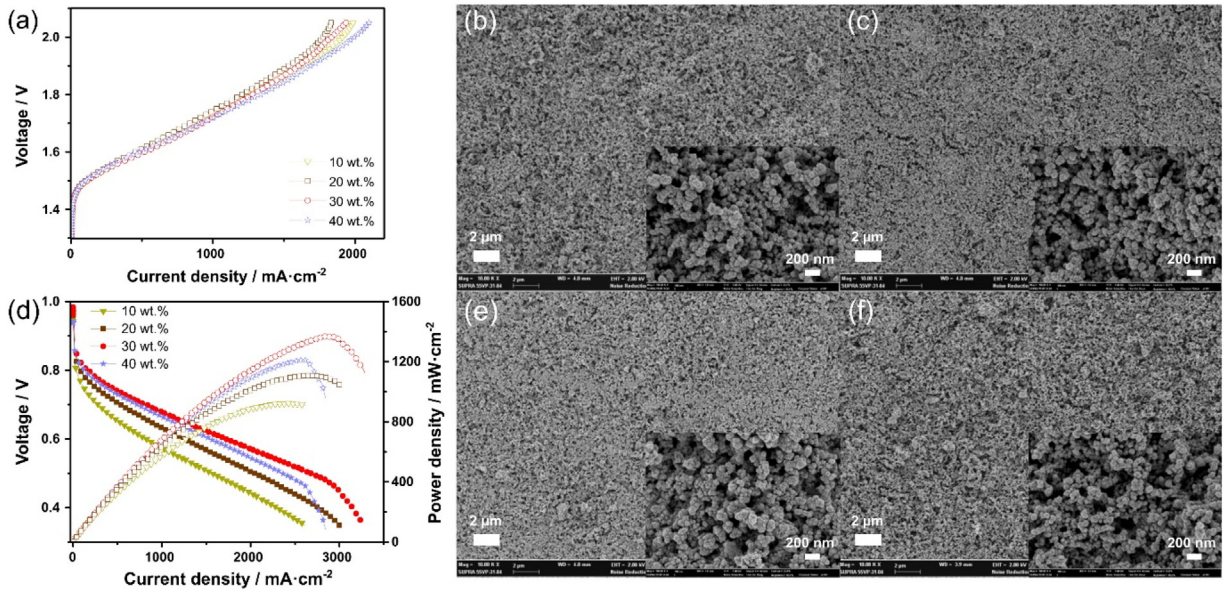

Fig. 4. The effect of ionomer contents (a, d) polarization curves of the URFCs prepared using different Nafion contents in the oxygen electrode in (a) WE and (d) FC mode and (b–f) FE-SEM images of the MEA with Nafion contents of (b) 10, (c) 20, (e) 30, and (f) 40 wt%.

Effect of ORR catalysts in the oxygen electrode

The oxygen electrode used in this study was comprised of a mixture of Pt- and Ir-based catalysts. For PEMFC, the Pt supported on carbon has been widely used as an ORR catalyst. The carbon support decreases the Pt nanoparticle size and offers high electrochemical surface area (ECSA) [30]. In addition, secondary pore formation caused by the presence of the carbon support resulted in enhanced mass transport, leading to improved PEMFC performance [31]. However, for PEMWE the carbon support is easily corroded under operating conditions owing to the high anodic potential. The IrO2 or Ir black catalyst without support have been widely used as OER catalysts in PEMWE. Therefore, it is important to determine the ideal carbon ratio in the ORR catalyst to simultaneously obtain high round-trip efficiency and low performance loss.

The effect of Pt-based catalysts with various Pt contents (20, 40, and 60 wt% Pt/C and Pt black) was examined by evaluating the resulting URFC performances. IrO2 black was maintained as the OER catalyst. Fig. 5(a) shows the polarization curves of the URFCs prepared with different ORR catalysts after 3 cycles and Fig. 5(c–f) shows the polarization curves of URFCs with (c) Pt black, (d) 60, (e) 40, and (f) 20 wt% Pt/C for 3 cycles. In WE mode, the MEA with Pt black exhibited the highest performance and stability among the Pt-based catalysts. The ohmic resistance of the URFC prepared with Pt black was smaller than that obtained using Pt/C catalysts, as shown in Fig. 6(a). The performance

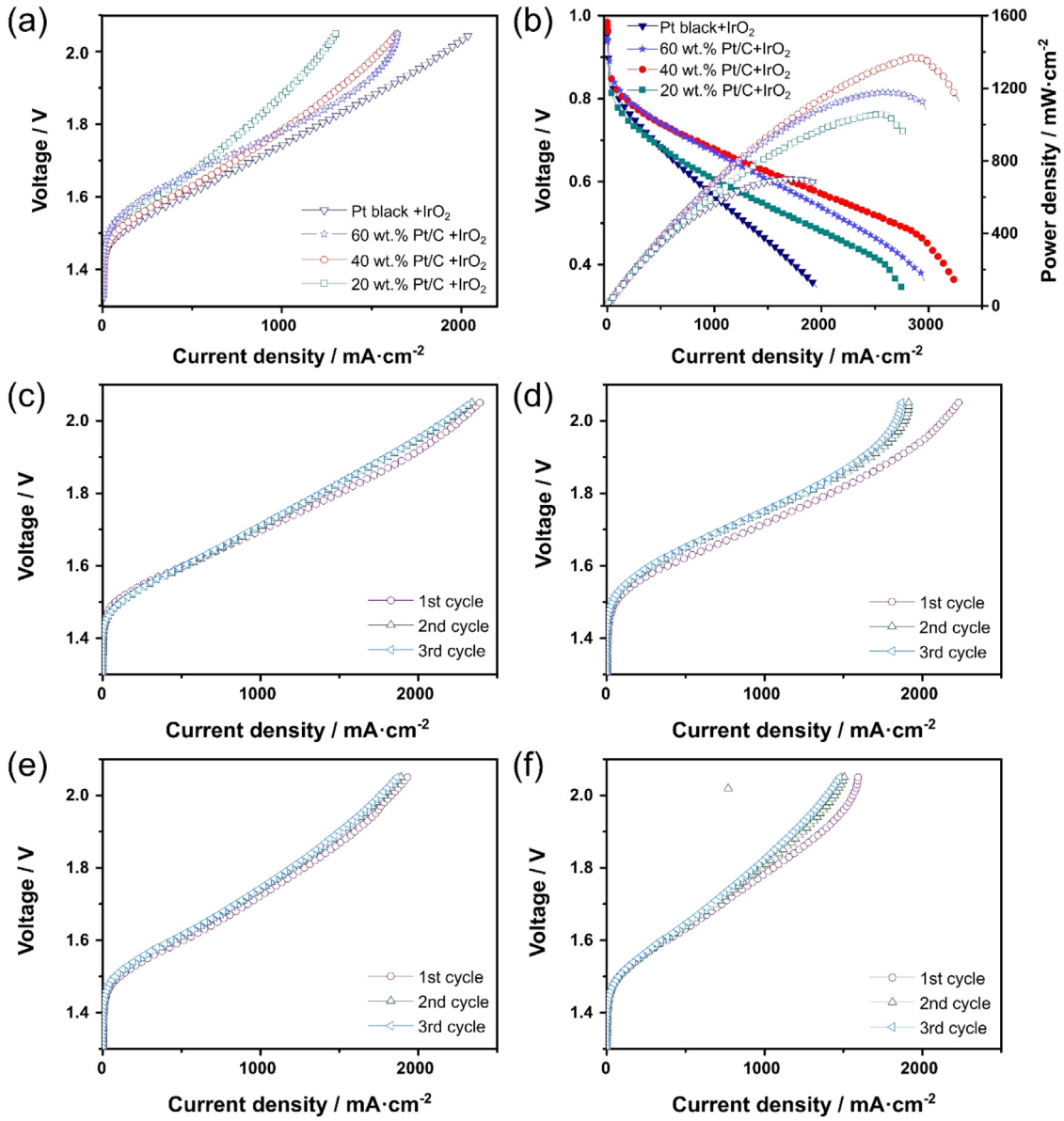

Fig. 5. The effect of ionomer contents (a, b) Polarization curves of URFCs prepared using different Nafion contents in the oxygen electrode in (a) WE and (b) FC mode. Polarization curves of the URFCs in WE mode using different ORR catalysts: (c) Pt black, (d) 60, (e) 40, and (f) 20 wt% Pt/C over 3 cycles.

losses at 500 mA cm^{-2} for 3 cycles were 0, 22, 18, and 25 mV for the device with Pt black, 60, 40, and 20 wt% Pt/C, respectively (Fig. 5(c–f)). Unlike the devices prepared with Pt black, the URFC with Pt/C exhibited performance loss. It is expected that the URFC performance in WE mode would be consistent regardless of the ORR catalyst type due to the constant OER catalyst. However, the four URFCs showed different performance. This result is ascribed to the different morphologies and thicknesses of the catalyst layers formed using different ORR catalysts (Fig. 6(b–f)). The catalyst layer with Pt black was thin and showed the lowest ohmic resistance. This demonstrates that WE performance is largely related to the ohmic resistance, which is largely governed by the thickness of the catalyst layer.

Fig. 5(b) shows the polarization curves of the URFCs with different ORR catalysts in FC mode. In FC mode, the MEA with Pt black exhibited the lowest performance because the catalyst layer without carbon support exhibited a dense morphology. Unlike Pt black, the MEA prepared with carbon supported Pt (20, 40, and 60 wt%) showed higher performance owing to the presence of the catalyst layer. In the low current density region, the cell performance increased with increasing Pt content due to smaller charge-transfer resistance and thinner catalyst layer, as shown in Fig. 6(b–f). On the other hand, the MEA with 40 wt% Pt/C exhibited the highest performance in the high current density region compared to those obtained with 20 and 60 wt% Pt/C. As shown in Fig. 6(c–f), secondary pores in the catalyst layer and catalyst layer thickness increased with increasing carbon content. For 60 wt% Pt/C, smaller secondary pores in the catalyst layer decreased mass transport despite the thin catalyst layer. For the 20 wt% Pt/C, although the catalyst layer contained larger secondary pores, the thicker catalyst layer led to decreased mass transport. Thus, the URFC prepared with 40 wt% Pt/C showed the highest overall FC performance considering all current density regions due to its catalyst layer morphology.

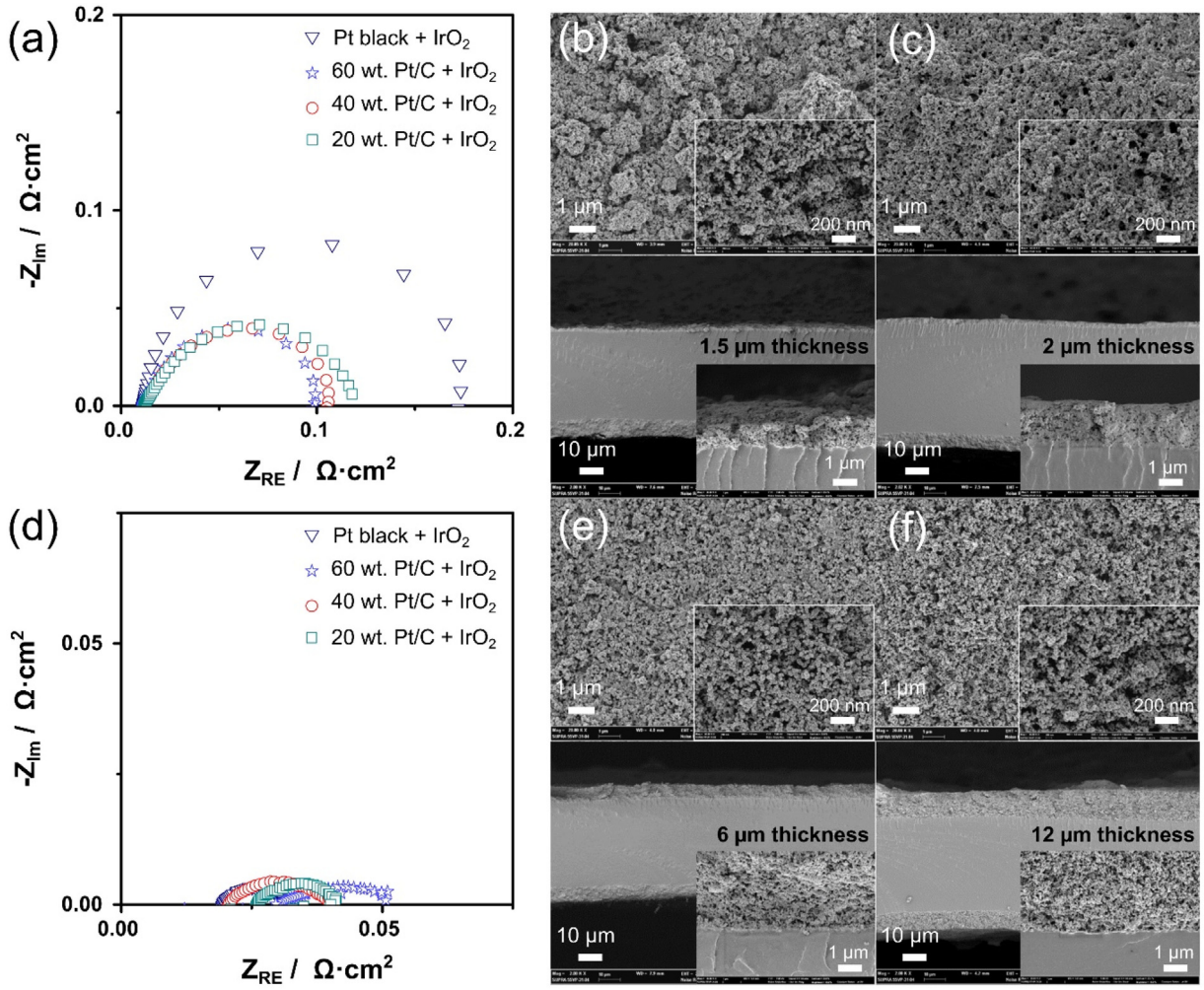

Fig. 6. Nyquist plots for URFC single cells with (a, d) different ORR catalysts. (a) FC mode and (d) WE mode. Nyquist plots were evaluated at –500 and 500 mA cm^{-2} in FC and WE modes, respectively. SEM images of the four MEAs prepared using different ORR catalysts: top view and cross-section view of MEAs with (b) Pt black, (c) 60, (e) 40, and (f) 20 wt% Pt/C.

To determine the ideal Pt to carbon ratio, the round-trip efficiency was calculated using the observed performances in FC and WE modes. The URFC potentials obtained in FC mode were 0.682, 0.741, 0.74, and 0.683 for Pt black, 60, 40, and 20 wt% Pt/C, respectively. The URFC performances evaluated in WE mode were 1.597, 1.653, 1.615, and 1.647 for Pt black, 60, 40, and 20 wt% Pt/C, respectively. The calculated round-trip efficiencies were 42.7, 44.8, 45.8, and 41.9% for Pt black, 60, 40, and 20 wt% Pt/C, respectively. Although the URFC with 60 wt% Pt/C showed the highest PEMFC performance and that with Pt black exhibited the highest PEMWE performance, the 40 wt% Pt/C exhibited the highest overall URFC performance. Thus, the 40 wt% Pt/C was determined to be the optimal ORR catalyst.

Effect of the OER catalysts in the oxygen electrode

Different OER catalysts, including Ir and IrO_2, were investigated to achieve high URFC performance. The Ir-based materials including the metal (Ir) and metal oxide (IrO_2) are well-known active OER electrocatalysts. While Ir exhibits higher OER activity than that of IrO_2, IrO_2 is more stable under acidic conditions with a low dissolution rate compared to that of Ir [32]. Fig. 7(a, b) shows the URFC performance in both FC and WE modes. While the ORR catalyst type significantly affected WE performance, the FC performances of the prepared URFCs with different OER catalysts showed similar performances and resistances, as shown in Fig. 7(a) and 8 (a). This is likely due to the similar morphology and catalyst layer thicknesses, as shown in Fig. 8(b–f). In contrast, the WE performance of the URFC prepared with Ir was higher than that of IrO_2, which is consistent with the literature [32]. This can be attributed to the low charge transfer resistance resulting from higher catalytic activity (Fig. 8(d)). The performance losses at 500 mA cm^{-2} were 30 and 18 mV for the Ir and IrO_2 catalysts, respectively, indicating that IrO_2 is more stable than Ir. Although Ir exhibits poor stability, the WE performance of the URFC prepared with Ir after 3 cycles (1.597 V) was lower than that of IrO_2 (1.615 V). As a result, the URFC with Ir showed the highest round-trip efficiency of 45.9 V.

Optimized cell performance of the URFC

As a result of the above investigations, Fig. 9(a) shows the optimal URFC performance operated in both FC and WE modes. The optimal URFC consists of an oxygen electrode prepared with 40 wt% Pt/C and Ir with a catalyst loading of 1.0 mg cm^{-2}, Nafion content of 30 wt%, and A3-30 GDLs. The URFC exhibited a high initial round-trip efficiency of 49% at 500 mA cm^{-2} (FC mode: 0.757 V and WE mode: 1.546 V).

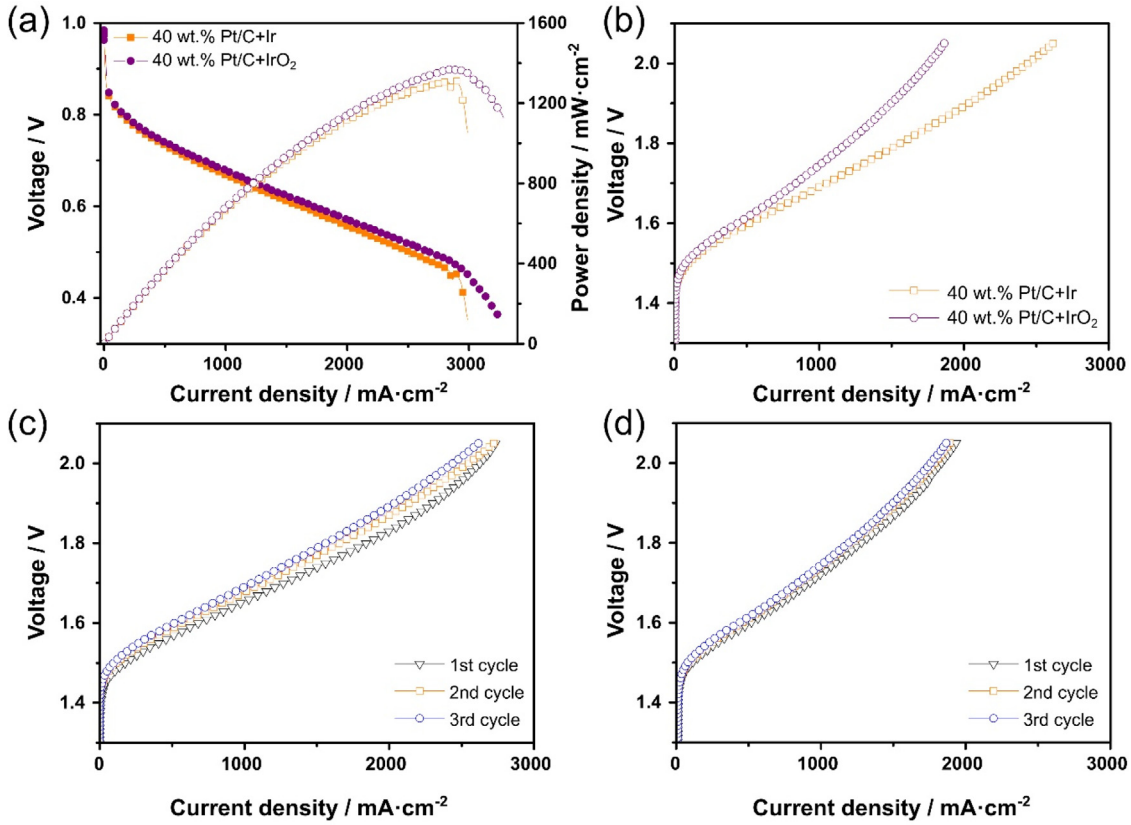

Fig. 7. Polarization curves of the URFCs prepared with different OER catalysts (Ir and IrO_2) in (a) FC mode and (b) WE mode. The short-term stability test in WE mode was conducted with (c) Ir and (d) IrO_2 catalysts for OER.

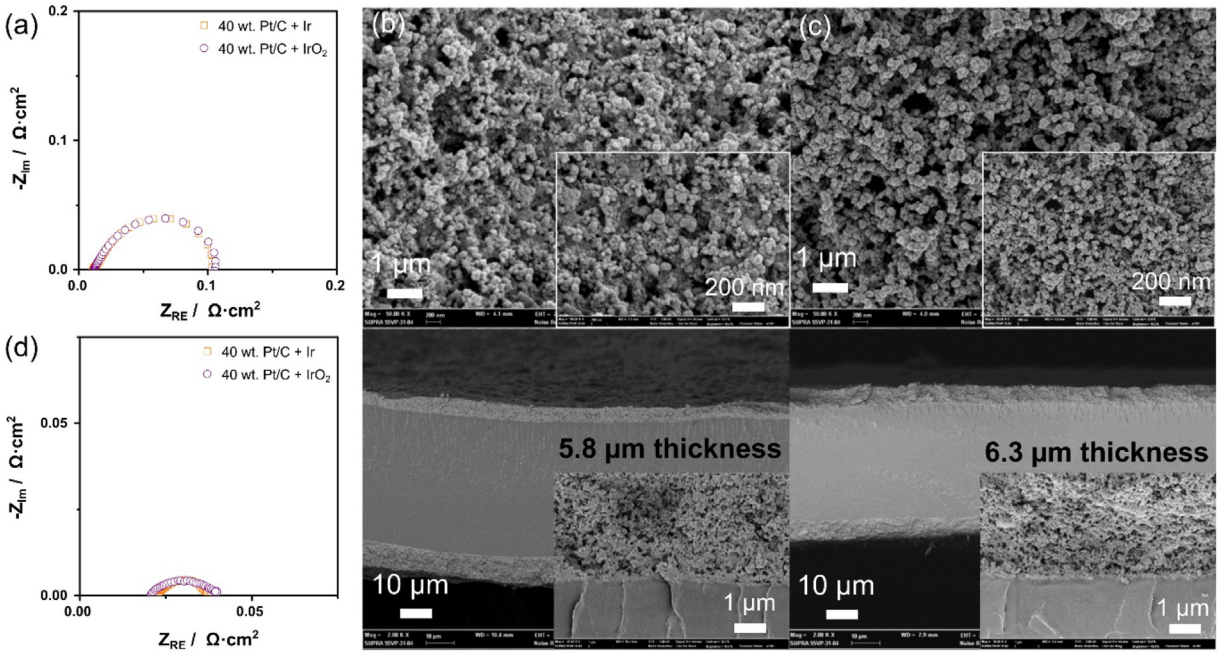

Fig. 8. Nyquist plots for URFC single cells with (a, d) different OER catalysts. (a) FC mode and (d) WE mode. Nyquist plots were evaluated at –500 and 500 mA cm^{-2} in FC and WE modes, respectively. SEM images of the two MEAs using different OER catalysts: top view and cross-section view of the MEAs with (a) Ir black and (b) IrO_2 black.

Fig. 9(b) and Table 1 show a comparison pf the round-trip efficiency of the optimized URFC with those reported in the literature [6–10,12]. The performance achieved herein is comparable or superior to previous reports. Except for novel catalyst layer structures [10], the URFC prepared herein exhibited high round-trip efficiency despite its low catalyst loading of 1 mg cm^{-2}. The optimization of the oxygen electrode in the URFC resulted in high performance by adjusting the parameters to be suitable for both FC and WE modes.

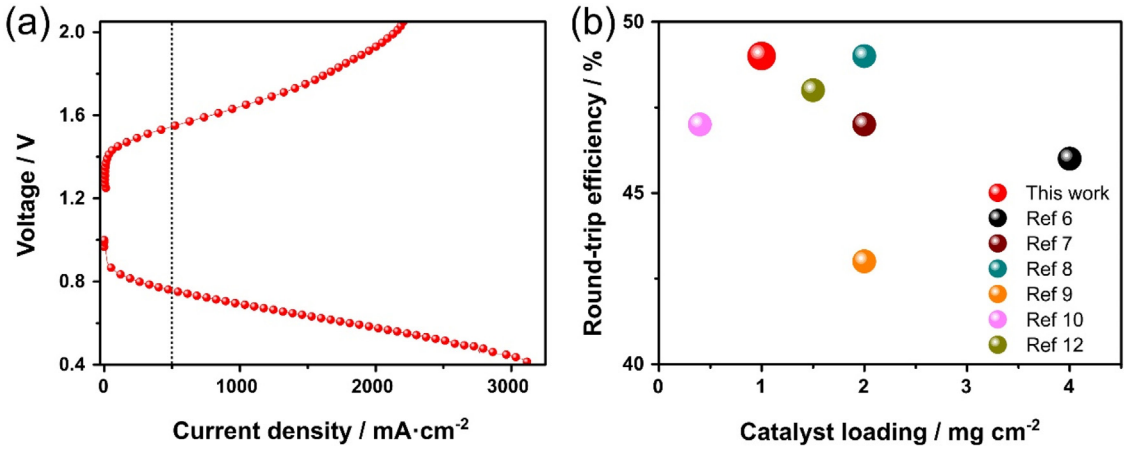

Fig. 9. (a) Optimized URFC performance in both FC and WE modes and (b) comparison with round-trip efficiencies reported in literature [6–10,12].

Table 1
Comparison of URFC performances (round-trip efficiencies) at 500 mA cm^{-2} reported in the literature and achieved in this study.

Catalyst	Catalyst loading (mg cm^{-2})	Round-trip efficiency (%)	Reference
40 wt.% Pt/C + Ir	1	49	This work
PtIr alloy (50:50)	4	46	[6]
PtIr alloy (99:1)	2	47	[7]
PtIr alloy (85:15)	2	49	[8]
(RuO_2–IrO_2)/Pt	2	43	[9]
Porous Pt/IrO_2/carbon paper	0.4	47	[10]
IrO_2/Pt/IrO_2 multilayer	1.5	48	[12]

Conclusion

In summary, the MEA parameters of the oxygen electrode in URF were adjusted to achieve high initial performance. Although only MEA parameters were adjusted to obtain high performance, they significant influenced URFC performance. The URFC performance was largely affected by the parameters that most influenced FC performance. The optimized URFC showed a high round-trip efficiency of 49% at constant current density of 500 mA cm^{-2}, which is comparable or superior to those obtained in previous studies. This study demonstrates and electrode structure that is suitable for a bifunctional catalyst to participate in both the ORR and OER and exhibit high initial performance. However, this URFC exhibits low durability due to its carbon support. Further investigation regarding corrosion-resistant supports, including graphitized carbon and titanium-based supports, is expected to increase cyclic performance.

Acknowledgments

This work was supported in part by the Institute for Basic Science (IBS) in Korea (IBS-R006-A2). This research was also supported by the Post-Doctor Research Program (2017) through Incheon National University (INU).

References

[1] Y. Wang, D.Y.C. Leung, J. Xuan, H. Wang, Renew. Sustain. Energy Rev. 65 (2016) 961.
[2] B. Paul, J. Andrews, Renew. Sustain. Energy Rev. 79 (2017) 585.
[3] T. Reier, M. Oezaslan, P. Strasser, ACS Catal. 2 (2012) 1765.
[4] S. Sui, X. Wang, X. Zhou, Y. Su, S.B. Riffat, C.-J. Liu, J. Mat. Chem. A 5 (2017) 1808.
[5] Y. Yan, B.Y. Xia, B. Zhao, X. Wang, J. Mater. Chem. A 4 (2016) 17587.
[6] S.-D. Yim, W.-Y. Lee, Y.-G. Yoon, Y.-J. Sohn, G.-G. Park, T.-H. Yang, C.-S. Kim, Electrochim. Acta 50 (2004) 713.
[7] S.-D. Yim, G.-G. Park, Y.-J. Sohn, W.-Y. Lee, Y.-G. Yoon, T.-H. Yang, S. Um, S.-P. Yu, C.-S. Kim, Int. J. Hydrogen Energy 30 (2005) 1345.
[8] H.-Y. Jung, P. Ganesan, B. Popov, ECS Trans. 25 (2009) 1261.
[9] Y. Zhang, C. Wang, N. Wan, Z. Mao, Int. J. Hydrogen Energy 32 (2007) 400.
[10] B.-S. Lee, H.-Y. Park, M.K. Cho, J.W. Jung, H.-J. Kim, D. Henkensmeier, S.J. Yoo, J.Y. Kim, S. Park, K.-Y. Lee, J.H. Jang, Electrochem. Commun. 64 (2016) 14.
[11] S. Altmann, T. Kaz, K.A. Friedrich, Electrochim. Acta 56 (2011) 4287.
[12] W.H. Lee, H. Kim, J. Electrochem. Soc. 161 (2014) F729.
[13] X. Huang, W.A. Rigdon, K.J. Billings, T.I. Valdez, ECS Trans. 50 (2013) 753.
[14] P.T. Babar, A.C. Lokhande, M.G. Gang, B.S. Pawar, S.M. Pawar, J.H. Kim, J. Ind. Eng. Chem. 60 (2018) 493.
[15] A. Lim, H.-J. Kim, D. Henkensmeier, S.J. Yoo, J.Y. Kim, S.Y. Lee, Y.-E. Sung, J.H. Jang, H.S. Park, J. Ind. Eng. Chem. 76 (2019) 410.
[16] J.E. Park, M.J. Kim, M.S. Lim, S.Y. Kang, J.K. Kim, S.H. Oh, M. Her, Y.H. Cho, Y.E. Sung, Appl. Catal. B: Environ. 237 (2018) 140.
[17] J.E. Park, S. Kim, O.H. Kim, C.Y. Ahn, M.J. Kim, S.Y. Kang, T.I. Jeon, J.G. Shim, D.W. Lee, J.H. Lee, Y.H. Cho, Y.E. Sung, Nano Energy 58 (2019) 158.
[18] S. Park, J.-W. Lee, B.N. Popov, Int. J. Hydrogen Energy 37 (2012) 5850.
[19] Z. Kang, J. Mo, G. Yang, S.T. Retterer, D.A. Cullen, T.J. Toops, J.B. Green Jr., M.M. Mench, F.-Y. Zhang, Energy Environ. Sci. 10 (2017) 166.
[20] H. Choi, O.H. Kim, M. Kim, H. Choe, Y.H. Cho, Y.E. Sung, ACS Appl. Mater. Interfaces 6 (2014) 7665.
[21] A. El-Kharouf, N.V. Rees, R. Steinberger-Wilckens, Fuel Cells 14 (2014) 735.
[22] B.-S. Lee, S.H. Ahn, H.-Y. Park, I. Choi, S.J. Yoo, H.-J. Kim, D. Henkensmeier, J. Y. Kim, S. Park, S.W. Nam, K.-Y. Lee, J.H. Jang, Appl. Catal. B: Environ. 179 (2015) 285.
[23] P. Ferreira-Aparicio, A.M. Chaparro, Adv. Energy Res. 2 (2014) 73.
[24] Q. Guo, M. Cayetano, Y.-m. Tsou, E.S. De Castro, R.E. White, J. Electrochem. Soc. 150 (2003) A1440.
[25] D. Lee, S. Hwang, Int. J. Hydrogen Energy 33 (2008) 2790.
[26] S. Litster, G. McLean, J. Power Soc. 130 (2004) 61.
[27] E. Passalacqua, F. Lufrano, G. Squadrito, A. Patti, L. Giorgi, Electrochim. Acta 46 (2001) 799.
[28] A. Suzuki, U. Sen, T. Hattori, R. Miura, R. Nagumo, H. Tsuboi, N. Hatakeyama, A. Endou, H. Takaba, M.C. Williams, A. Miyamoto, Int. J. Hydrogen Energy 36 (2011) 2221.
[29] X. Wu, K. Scott, Int. J. Hydrogen Energy 35 (2010) 12029.
[30] E. Antolini, Appl. Catal. B: Environ. 88 (2009) 1.
[31] Z.A.C. Ramli, S.K. Kamarudin, Nanoscale Res. Lett. 13 (2018) 410.
[32] S. Cherevko, S. Geiger, O. Kasian, N. Kulyk, J.-P. Grote, A. Savan, B.R. Shrestha, S. Merzlikin, B. Breitbach, A. Ludwig, K.J.J. Mayrhofer, Catal. Today 262 (2016) 170.